Characterization of structural reorganization in rice piles

K. I. Hopcraft, E. Jakeman, and R. M. J. Tanner
Theoretical Mechanics Division, School of Mathematical Sciences, University of Nottingham, University Park, Nottingham, NG7 2RD, United Kingdom
(Received 8 February 2001; published 19 June 2001)

Diagnostics applied to a rice-pile cellular automaton reveal different mechanisms producing power-law behaviors of statistical attributes of grains which are germane to self organised critical phenomena. The probability distributions for these quantities can be derived from two distinct random walk models that account for correlated clustered behavior through incorporating fluctuations in the number of steps in the walk. The first model describes the distribution for a spatial quantity, the resultant flight length of grains. This has a power-law tail caused by grains moving through a discrete, power-law distributed number of random steps of finite length. Developing this model into a random walk obtains distributions for the resultant flight length with characteristics similar to Lévy distributions. The second random walk model is devised to explain a temporal quantity, the distribution of ''trapping'' or ''residence'' times of grains at single locations in the pile. Diagnostics reveal that the trapping time can be constructed as a sum of ''subtrapping times,'' which are described by a Lévy distribution where the number of terms in the sum is a discrete random variable accurately described by a negative binomial distribution. The infinitely divisible, two-parameter, limit distribution for the resultant of such a random walk is discussed, and describes a dual-scale power-law behavior if the number fluctuations are strongly clustered. The form for the distribution of transit times of grains results as a corollary.

DOI: 10.1103/PhysRevE.64.016116 PACS number(s): 02.50.−r, 89.75.Da, 05.65.+b

I. INTRODUCTION

Interest in self organized criticality (SOC) is multidisciplinary, and continues to burgeon (see, e.g., Ref. [1]). The concept of SOC refers to the spontaneous emergence of complexity in nonequilibrium systems that are nevertheless dynamically simple. Particular attention has been paid to the statistical mechanics of granular media and, as a consequence, the ''sandpile'' has become the touchstone of SOC. When a pile of sand is fueled by the addition of grains, it evolves into a state where, on average, the quantity of matter expelled from the pile is equal to the amount added to it. This dynamic equilibrium is maintained by an intermittent cascade of material down the pile through avalanches that exist on all scale sizes up to the dimensions of the system. This sandpile paradigm has prompted workers to characterize complex systems through a simplified dynamics where fueling is followed by reorganization once a local critical threshold is exceeded. The reorganization can lead to instability at other sites, and consequently can establish long-scale correlated behavior throughout the pile. The statistical description of the scale-invariant behavior that is obtained is typified by distributions possessing power-law tails, and in seeking a model for this, interest in the class of ''stable'' or ''Lévy'' distributions [2] has been rekindled.

SOC behavior was demonstrated experimentally in the celebrated ''Oslo rice pile'' [3], and its detailed dynamics was elucidated by investigating the motion of tracer grains. The distribution for the transit times of grains through rice piles of variable size exhibited, on the longest scales, a decaying power law extending over approximately two decades. The data show a second region of power-law behavior an the shortest time scales for smaller sized rice piles, although the authors did not comment upon this. A cellular automaton that purported to model this rice pile [4] also exhibited a dual power law at short and long scales for the distribution describing the trapping time of grains, but again the authors confined their attention and discussion to the tail of the distribution, modeling it with Lévy statistics. A dual power-law behavior cannot be described using Lévy statistics, which can only characterize the power law featured on the largest scales. One aim of this paper is to deconstruct the temporal behavior produced by the cellular automaton, and describe it in terms of a random walk model which has, as a key ingredient, fluctuations in the number of steps forming the walk, as in Ref. [5]. This is motivated by the well known technique [6] by which correlation may be introduced into a random walk through fluctuations in the number of steps, meaning that successive realisations of the walk contain different numbers of steps *independent of the properties of the step lengths*. This allows a sequence of events to be clustered (correlated) in time, for example, although their individual contribution to the quantity of interest are unrelated to the clustering process. A consequence of this is that the dual power-law behavior for trapping times occurs naturally and, moreover, predicts the observed form for the distribution of transit times. It was also shown in Ref. [4] that the distribution of flight lengths of grains could be modeled using Lévy statistics. This raises the paradox that a spatial transport quantity can have arbitrarily large excursions, which apparently conflicts with constraints imposed by the energetics of the system. Another aim of this paper is to resolve this paradox by showing that a grain's flight is comprised of a fluctuating number of ''subflights'' of finite length, where the number of subflights is described by a discrete power law. This notion leads to flight lengths possessing the attributes of a Lévy distribution without the attendant problem of unphysical energetics.

Cellular automata provide an important tool for the investigation of the dynamics of sand piles. Based on a few el-

ementary rules, they have enabled a prediction of macroscopic behaviors that can and have been observed in real systems, and advanced the knowledge of the microscopic dynamics involved. However, the choice of model has not been related closely to the properties of any individual system, since the objectives have, to date, been principally to illuminate the generic processes leading to SOC and their overall outcome. To make quantitative predictions of a practical nature, it is important to understand in greater detail how the microscopic reorganizations of the system are related to the assumed numerical model. This would enable a more realistic modeling of both naturally occurring and synthesized phenomena to be achieved in the future. As a response to this, this paper presents a detailed statistical analysis of the internal reorganizations of a sand pile predicted by an established cellular automaton. This provides further insight into the relevance of random walk models to the subject, and emphasizes the importance of discrete number fluctuations as a descriptor and motor for the dynamics.

This paper first reviews the cellular automaton used to describe the rice-pile experiment, describing in particular the physical structure of the pile in the self-organized state and how this structure influences the various behaviors of tracer grains transported through the pile. Section III concentrates on a spatial property, the distribution of flight lengths, and illustrates how these can be deduced from a random walk model where the number of steps in the walk fluctuates with a discrete power-law distribution. Section IV focuses on temporal properties, and presents evidence that the trapping time distribution can also be understood using a random walk model, but where now the individual steps in the walk are Lévy distributed time increments and the number of steps is a negative binomial random variate. This distribution is then used to derive the observed form of the transit time distribution of tracer grains. Section V summarizes and discusses the implications of this work. Technical details pertaining to the derivations and forms of the distributions are assigned to appendixes.

II. RICE-PILE CELLULAR AUTOMATON

The cellular automaton studied in Ref. [4] was designed to replicate experimental data of the Oslo rice pile reported in Ref. [3], and has the advantage of being able to track and apply diagnostics to test particles as they move throughout the pile. The automaton therefore enables microscopic properties of particles and macroscopic attributes of the entire pile to be studied simultaneously.

The cellular automaton examines the stability of a set of slopes z_m in excess of an angle of repose, where $1<m<L$ labels a spatial position within the pile. If the slope attains a critical gradient z_m^c at site m, ''sand'' is redistributed in such a way that the gradient is reduced to a subcritical value there and raised at nearest neighbor sites according to the rule $z_m \geqslant z_m^c \Rightarrow z_{m-1} \rightarrow z_{m-1}+1,\ z_m \rightarrow z_m-2,\ z_{m+1} \rightarrow z_{m+1}+1$. The critical gradient at a site is a Bernoulli random variable that fluctuates between 1 and 2 with equal probability, being reassigned whenever a grain passes over that site. Special conditions apply at the end of the pile, where the rule is modified

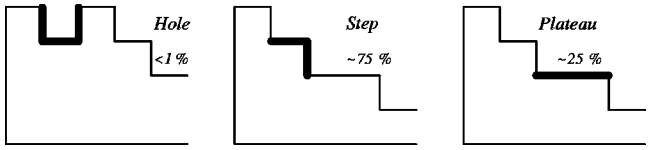

FIG. 1. The essential elements from which a sand pile is comprised, together with the frequency of occurrence.

so that if $z_L \geqslant z_L^c,\ z_{L-1} \rightarrow z_{L-1}+1,\ z_L \rightarrow z_L-1$. The redistribution of grains at unstable sites occurs sequentially, counting from the left to the right of the pile, in accordance with causality. Iteration throughout the pile continues until it attains a state with $z_m<z_m^c$ everywhere. The pile is then fueled at the top, so that $z_1 \rightarrow z_1+1$, and the process continues. The toppling rule of the automaton used here differs slightly from that used in Ref. [4], where the condition was $z_m>z_m^c$, which necessarily has fewer toppling events and results in a ''steeper'' pile. This alteration does not affect the statistical properties of the tracer grains, but has the advantage of being more efficient computationally, and therefore allows more sophisticated diagnostics to be applied. The simplicity of the algorithm belies the complexity of behavior it describes.

Two diagnostics were used in Ref. [4] to characterize behavior: the ''flight length'' and ''trapping-time'' distributions of grains. To understand how the empirical results quoted in Ref. [4] arise and become quantifiable in terms of two distinct but simple stochastic models, diagnostics have to be applied to the cellular automaton that elucidate the statistical mechanics of the ensemble of grains. The way that these diagnostics inform the construction of these models is best appreciated by describing some aspects of the cellular automatons behavior.

A pile in the self-organized state forms a sequence of ''staircases'' interspersed with ''plateaus'' and, less frequently, ''holes.'' These elements are illustrated in Fig. 1. The algorithm predicts that a stable SOC pile has an average slope $\sim 3/4$, and so $\sim 75\%$ of the piles' surfaces comprise sections of staircase, $\sim 25\%$ plateaus, with holes occurring with a frequency $<1\%$. The distance between consecutive plateaus is approximately exponentially distributed, with a mean interplateau spacing $\Delta l \sim 4$ grain sites, and most plateaus have a length of two sites. Thus a stable pile of total length 400 has about 100 plateaus randomly distributed through it. The algorithm proceeds by the addition of a grain to the first site of such a pile. The stability of this site is tested and, if unstable, the grain moves to the next site, and so on, until coming to rest. Grains must necessarily move down a staircase section, and so the principal location at which a grain can come to rest is a plateau. Such a potential resting site has a random preassigned critical slope associated with it. If this is 1, the grain continues to the next potential resting site on the same or at the next plateau. If the critical slope is 2, the grain ''sticks.'' In those rare instances when a grain falls into a hole, it sticks with probability 1 and forms a new plateau. Holes rapidly fill, accounting for their infrequent occurrences. Because the critical slope is either 1 or 2 with equal probability, a grain has an average subflight length of two interplateau distances, or approximately eight-

grain sites before it comes to rest at a plateau. All the sites over which this grain has passed (staircases and plateaus alike) are ''perturbed'' by randomly reassigning their critical slopes. Hence the potential exists for one of these sites, which was initially stable, to be transformed to an unstable site (and vice versa). An unstable site will shed a grain, causing another subflight to ensue and continue the ''avalanche.'' The order in which the stability of sites is tested always increases away from the top, effectively running down the surface of the pile. Hence there is an ''active zone'' defining the spatial extent between where grains commence and terminate their subflights: it denotes the location of the avalanche at any instant, and is purely a surface feature. With each grain's subflight, the active zone fluctuates in position within the pile and in length, the latter necessarily evolving to zero as the pile returns to a state of global stability. It is the position of the rear of the active zone (i.e., closest to the top of the pile) that determines whether a tracer grain has the opportunity for another subflight. The next time that the rear of the active zone passes over such a grain at the surface of the pile, it has the opportunity to move on another subflight.

One aspect to note is that the algorithm contains disparate time scales. The ''long'' time scale characterizes the fueling of grains which occurs between the pile being in two consecutive stable states. The ''short'' time scale characterizes the redistribution of all those grains that move between fueling events, and therefore fluctuates between successive addition of grains in accordance with the size of avalanche that is produced. Despite this, the avalanche is considered to occur instantaneously on the long time scale.

III. DISTRIBUTION OF FLIGHT LENGTHS

Section II described an active zone, which denotes the location and spatial extent of the avalanche and occurs on the short time scale. The feature of this structure that dictates whether or not an avalanche persists is the location of the rear of the active zone m_a; as this moves over tracer grains, its action provides them with the opportunity to move off to the next place of residence. Figure 2 shows the probability distribution for m_a for a pile of length $L=1000$. The distribution is a power law over three decades with index -0.8. The feature appearing at small values of m_a is due to special conditions that prevail near the fueling point, and the cutoff at largest scales is due to the finite length of the system. This very shallow power law implies that the active zone has no mean location. Therefore, it can move anywhere over the entire pile, triggering grains to move as it does so. Indeed, this must be so, for a tracer grain would hardly ever be expelled from the pile unless the active zone could explore every part of it. Thus a property of individual grains is influenced by a macroscopic structure of the pile. A grain has the opportunity to move many times within an avalanche as m_a moves back and forth. Moreover, this spatial movement causes the excavation of interred tracer grains which affect the temporal behavior of the pile, as will be explored in Sec. IV.

Figure 3 shows the probability distribution for N_s, the number of subflights of length l_i that cause a total avalanche

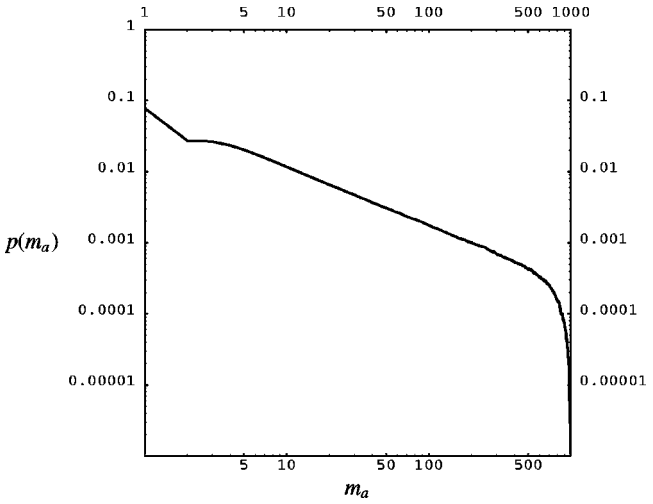

FIG. 2. The probability density for the location for the rear of the active zone m_a for a pile of length $L=1000$. The distribution is a power law with index -0.8, and is normalizable only by virtue of an end effect. The distribution for m_a has the same power law for smaller pile lengths.

flight of length l for a pile of size 400 sites. The flight length $l=\sum_{i=1}^{N_s} l_i$ is the total distance traveled by a grain between fueling events, and fluctuates with N_s and l_i. The distribution shown is for tracer grains emanating from site 2 of the pile, principally because these have the potential for the longest flights. This discrete distribution is a power law of index -2.14. The cutoff at $N_s \sim 100$ is due to the finite size of the pile. The reasons for the discrepancy between the indices of the power laws for N_s and m_a are complex. A grain does not necessarily move on another subflight when m_a passes over it; rather it has the *opportunity* to move. For example, the critical slope may have been reassigned to site 2, or the grain may be buried below the surface, in which case the grain will not or cannot move. Moreover the distribution for N_s is constructed as an ensemble average over all

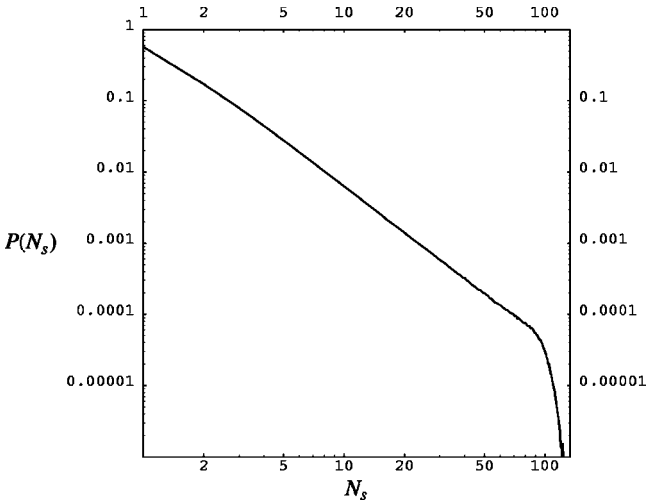

FIG. 3. The distribution for the number of subflights N_s for a pile of length $L=400$, which is a power law with index $\beta=-2.14$.

realizations of resultant flight lengths l. There are many combinations of subflights l_i comprising a given resultant flight l, and the probability for occurrence for these individual realizations would require enumeration if a match were sought. For the purpose of this paper it is sufficient to note that the underlying reason for the power law in N_s derives from the power law for m_a. It will now be shown how the above empirical observation that a tracer particle receives a power-law distributed number of ''kicks'' is used to obtain the distribution for l which matches the cellular automaton data. It will be shown that the resultant of the random walk is also a power law distribution with the same exponent as the number fluctuations.

In Sec. II the motion of grains was described as being a series of ''jumps'' or subflights which have an average length of eight sites, being two interplateau lengths. The actual distribution of interplateau lengths matters little to what follows, and can be taken as constant. The subflights can then be considered as integer multiples of a fixed interplateau length Δl, so that $l_n = n\Delta l$. Suppose that the probability of traversing any possible resting site is $1/\mu$, where $\mu > 1$. For the cellular automaton, $\mu = 2$, because the critical slope at the site of rest adopts one of two values. The probability of the grain travelling over $n-1$ independent potential resting sites before remaining at the nth site is therefore $(1/\mu)^{n-1}(1-1/\mu)$. Hence the generating function for obtaining a subflight of length l_n is

$$q(s) = \langle \exp(-s l_n) \rangle = (\mu - 1) \sum_{n=1}^{\infty} \left(\frac{1}{\mu} \right)^n \exp(-ns\Delta l)$$

$$= \frac{\mu - 1}{\mu \exp(s\Delta l) - 1}.$$

The form of the generating function near $s = 0$ determines the large-scale asymptotic behavior, i.e.,

$$q(s) \sim \frac{1}{1 + \mu s \Delta l/(\mu - 1)},$$

which is the generating function of the exponential distribution. A random walk comprising N_s such independent subflights has a resultant

$$l = \sum_{n=1}^{N_s} l_n, \tag{1}$$

with a generating function $q_N(s) = q(s)^N$, and this generates the gamma distribution

$$p_{N_s}(l) = \left(\frac{(\mu - 1) l}{\mu \Delta l} \right)^{N_s - 1} \frac{(\mu - 1)}{\mu \Delta l \Gamma(N_s)} \exp\left(- \frac{(\mu - 1) l}{\mu \Delta l} \right),$$

all moments of which exist. The model adopted for the number fluctuations that is consistent with Fig. 3 is taken to be

$$P(N_s) = \frac{1}{\zeta(\beta) N_s^{\beta}}, \quad N_s \geqslant 1, \quad \beta > 1 \tag{2}$$

where the Riemann zeta function $\zeta(\beta)$ [7] provides normalization. In approximating the rice pile behavior, it is assumed that the number of steps is independent of the length of each step. The distribution for the resultant flight length l that results from averaging over all realizations of N_s is

$$p(l) = \sum_{N_s = 1}^{\infty} P(N_s) p_{N_s}(l)$$

$$= \frac{(\mu - 1) \exp[-(\mu - 1) l/\mu \Delta l]}{\mu \Delta l \zeta(\beta)}$$

$$\times \sum_{N=0}^{\infty} \left(\frac{(\mu - 1) l}{\mu \Delta l} \right)^{N_s} \frac{1}{N_s! (1 + N_s)^{\beta}}.$$

Setting $x = (\mu - 1) l/\mu \Delta l$ obtains

$$p(x) = \frac{\exp(-x)}{\zeta(\beta)} \sum_{N_s = 0}^{\infty} \frac{x^{N_s}}{N_s! (1 + N_s)^{\beta}}. \tag{3}$$

An alternative expression for this probability density functions (PDF) can be obtained on using the definition of the gamma function [7], to write

$$(1 + N_s)^{-\beta} = \frac{1}{\Gamma(\beta)} \int_0^{\infty} du u^{\beta - 1} \exp[-(1 + N_s) u],$$

whereupon the summation can be evaluated to obtain the equivalent integral representation for the PDF [Eq. (3)]:

$$p(x) = \frac{\exp(-x)}{\zeta(\beta) \Gamma(\beta)} \int_0^{\infty} du u^{\beta - 1} \exp(-u) \exp[x \exp(-u)]. \tag{4}$$

This distribution, expressed either in the form of Eqs. (3) or (4) constitutes the first principal result of this paper.

The behavior of Eq. (4) is still not particularly evident, but can be made transparent by writing the ''exponential of an exponential'' as [8,5]

$$\exp[x \exp(-u)] \approx 1 + [\exp(x) - 1] \exp\left(- \frac{xu}{[1 - \exp(-x)]} \right),$$

which has the advantage of reducing to the conventional steepest descent approximation for large x, and is correct for arbitrary values of x if u is sufficiently small. Use of this approximation therefore yields the correct asymptotic behavior for large and small values of x. The remaining integrals are straightforward to perform, and give

$$p(x) \sim \frac{\exp(-x)}{\zeta(\beta)} + \frac{[1 - \exp(-x)]^{1 + \beta}}{\zeta(\beta)[1 - \exp(-x) + x]^{\beta}}$$

as an approximation for the PDF [Eqs. (3) and (4)] which conveniently reveals its structure. If x is small, $p(x) \sim 1/\zeta(\beta)$, whereas if x is large, the distribution has a power-law tail with $p(x) \sim 1/x^{\beta}$. In Appendix A it is shown that the asymptotic form of the tail can be determined with greater precision to be

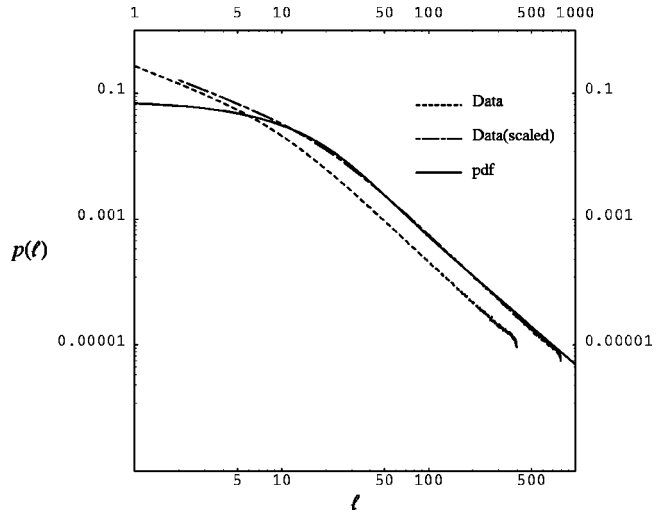

FIG. 4. The dashed curve is the distribution of flight lengths obtained from the cellular automaton for a pile of length $L=400$. The linearly scaled data are shown by the chain curve, and are compared with the distribution given by Eq. (3), shown by the full curve.

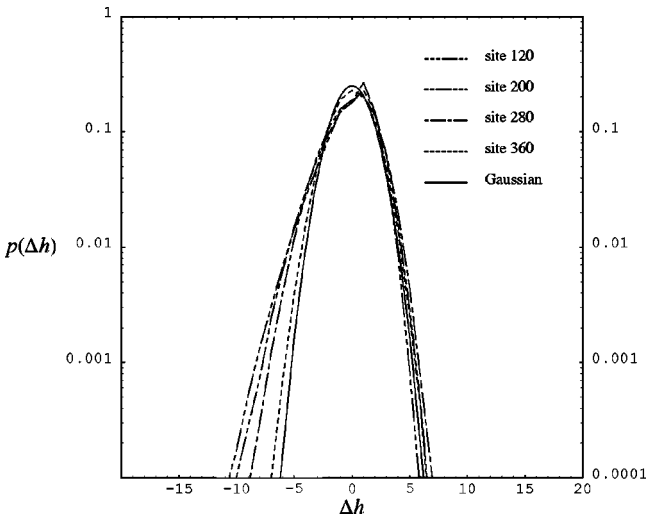

FIG. 5. Showing the fluctuations in height for different locations in the pile on a semilogarithmic plot. The curve codes are annotated on the figure with the Gaussian for comparison.

$$p(x)\sim\frac{1}{\zeta(\beta)x^{\beta}}\left(1+\frac{3+4(\beta+1/2)(\beta-3/2)}{8x}+\cdots\right) \quad (5)$$

when $x\gg 1$. The rth moment of Eqs. (3) and (4) exists only if $r<\beta-1$, a property inherited from the parent distribution [Eq. (2)]. In particular, a mean flight length $\langle l\rangle$ exists if $\beta>2$, and an elementary calculation obtains

$$\langle l\rangle=2\Delta l\frac{\zeta(\beta-1)}{\zeta(\beta)}, \quad (6)$$

and so a grain moving through a pile of total length L has on average $\overline{M}=L/\langle l\rangle$ flights before leaving the system.

The distinction between the distribution describing this random walk and a Lévy distribution is important to clarify, even though they ostensibly appear to have similar asymptotic forms. The power-law tail in a Lévy random walk occurs as a consequence of the power-law distributed individual step lengths. Lévy random walks are inappropriate for describing, for example, the spatial movement of material where the energetics would prohibit the occurrence of arbitrary sized step lengths. In such instances it is more appropriate for the individual steps to have finite integer moments, but with the power-law behavior for the resultant ultimately deriving from another mechanism such as number fluctuations. Moreover, the index of the power law appearing in Eq. (2) is evidently not restricted to lie in the range for that of the stable distributions.

The dashed curve in Fig. 4 shows the distribution of l obtained from the cellular automaton for all grains emanating from site 2 of the pile. This has a power-law tail with index -2.14, and can be readily explained using the information contained in Fig. 3 together with the random walk described above. The full curve shows the distribution [Eq. (3)] where $\Delta l=4$ has been used, in accord with the value deduced from the average slope of a SOC pile. The chain curve is a simple linear scaling of the data, $p(l)\rightarrow 0.6p(2l)$. The agreement for large flight lengths is excellent, and the discrepancy at short flight lengths results from the simplifying assumption of uniform interplateau distances that was used to derive Eq. (3).

IV. DISTRIBUTION OF TRAPPING TIMES AND TRANSIT TIMES

The second diagnostic used in Ref. [4] was the distribution of ''trapping times,'' which is the time a grain remains at rest at a particular site. The trapping time occurs on the long time scale that is characterized by the rate of fueling. Each site is monitored to give a distribution of trapping times for the pile as a whole, and it was found that this distribution has a power-law tail and other features for which the following model can account.

A grain has the opportunity to move, and thereby end a trapping-time period, only if it is on the surface. Grains that are buried must wait until they are excavated. Figure 5 shows the distribution for increments in height Δh of the pile at different locations removed from the central fueling point. The increments are essentially stationary and have zero mean, but they are skewed and so deviate from a Gaussian distribution, which is also shown in the figure. Supposing for the moment that the distribution of height fluctuations are approximated by a Gaussian distribution, the instances when a particular grain returns to the surface may then be interpreted as the first return time of a Brownian fractal. The distribution for such a return time has a power-law tail [9]. In fact, because the height fluctuations are distinct from a Gaussian leads to being able to quantitatively determine the index of the power-law tail. However, the execution of this calculation itself requires a number of technical innovations which have a currency beyond applications to sand piles, and so the details were presented elsewhere [12]. For the purposes of this paper, it is entirely correct to model the time t_m

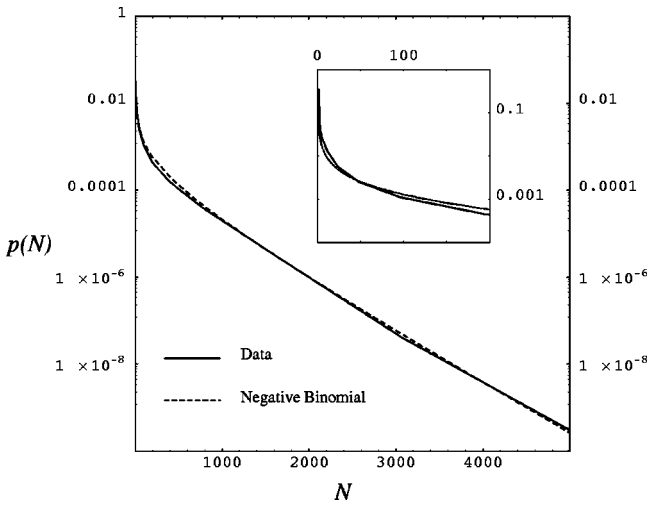

FIG. 6. The full curve shows the probability density for the number of instances that a grain is exposed at the surface of the pile but does not move, derived from cellular automaton data. The dashed curve is the negative binomial distribution with $\overline{N}=80$ and $\alpha=0.2$. Both are shown on semilogarithmic plots. The inset resolves the PDF for smaller numbers of exposures.

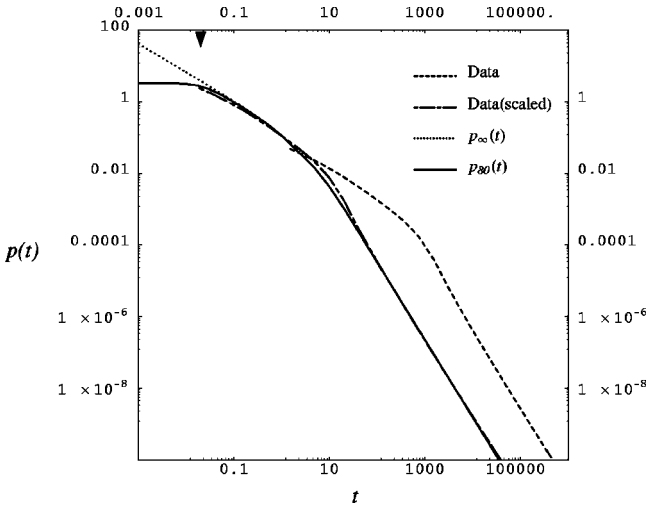

FIG. 7. The dashed curve shows the trapping time distribution for the cellular automaton, which is then linearly scaled given by the chain curve for comparison with the limit distribution (12) shown in full. The curve shows the PDF for finite $\overline{N}$, which introduces an inner scale indicated by the thorn on the upper axis. The values of $\alpha=0.2$ and $\overline{N}=80$ are those derived from the PDF illustrated in Fig. 6.

for a grain to return to the surface with a Lévy distributed random variable. The index of the distribution used will be obtained empirically from the cellular automaton simulation.

Although it is necessary for a grain to be on the surface for a trapping time to end, this requirement is not sufficient. The disinterred grain may be at a stable site, or may be buried again before having the opportunity to move. Thus a trapping time t comprises a sum of separate Lévy distributed time increments t_m between a grain remaining or returning to the surface, viz.

$$t=\sum_{m=1}^{N} t_m, \tag{7}$$

where N denotes the number of instances that a grain is exposed at the surface of the pile but does *not* move. The trapping time ends when the grain comes to the surface and *does* move. The dashed curve in Fig. 6 illustrates the PDF for N as obtained from the cellular automaton. The dashed curve is the negative binomial distribution [10]

$$P(N)=\binom{N+\alpha-1}{N}\frac{(\overline{N}/\alpha)^N}{(1+\overline{N}/\alpha)^{N+\alpha}}, \tag{8}$$

with a mean number of steps $\overline{N}=80$ and a clustering parameter $\alpha=0.2$. Remarkably, the data are indistinguishable from this model over three decades of values for N, and the inset shows that the model is accurate at very small values of N also. The reason why the number of resurfaces and reburials of a tracer grain at the surface of the pile should be accurately described by the negative binomial distribution is unclear, but the empirical evidence is compelling. Distribution (8) has two parameters: $\overline{N}$ is the mean and $\alpha>0$ is the cluster parameter. The special case $\alpha=1$ is the Bose-Einstein or geometrical distribution, which describes ''thermal'' number fluctuations, and $\alpha\to\infty$ is the Poisson distribution describing a purely random number of steps. The smaller the value of α, the greater the strength of the clustering. Insofar as the statistical description of clustering is an inherent feature of the distribution, it is again appropriate to use it in a variable step-number random walk to incorporate the effect of correlations. Bunching arises in the pile in the following qualitative fashion. Consider a system-wide avalanche in which a large number of tracer particles moves from, or resurfaces at, a particular site in the pile. Grains that have moved come to rest elsewhere, and therefore commence a new trapping time. Those that have resurfaced end their present trapping time and commence a new one. Thus a large set of grains simultaneously commences a fresh trapping time. After such an avalanche, successive fueling events tend to result in small sized avalanches confined to the top of the pile as the slope increases from a subcritical state. With each feed, all surface tracer grains at locations further down the pile receive identical time increments to their trapping times. Eventually the avalanches become larger and reach groups of surface tracer grains, bringing several trapping times to an end simultaneously. Many of these trapping times will comprise a similar number of time increments which provides the clustering in N.

These empirical facts will now be developed into a random walk model for the distribution of trapping times. The ingredients are individual ''subtrapping time'' increments t_m, which are power law distributed and can therefore be modeled by a Lévy distribution, together with a discrete number N of times that a grain comes to the surface of the pile without moving from that site, the statistics for which is described by Eq. (8). This model is similar to that introduced in Ref. [5]. The difference here is that the time increments t_m

are all positive, so that the theory must be recast in terms of the one-sided Lévy distributions to model t_m.

In Appendix B it is shown that using a one-sided Lévy distribution to describe the time increments with number fluctuations described by Eq. (8) obtains the following limit distribution for the trapping time on letting the average number of steps $\overline{N}\to\infty$:

$$p_{\alpha,\gamma}(t)=\mathrm{Re}\frac{1}{\pi}\int_0^\infty (1+u^\gamma(1+i\Lambda)/\alpha)^{-\alpha}\exp(iut)du, \tag{9}$$

where

$$\Lambda=\begin{cases}\dfrac{2}{\pi}\ln|u|, & \gamma=1\\ \tan(\gamma\pi/2), & \gamma\neq 1.\end{cases}$$

This density function is valid if the individual steps in the walk are drawn from the class of stable Lévy processes or from distributions having power-law tails *similar* to Lévy distributions, and it constitutes the second principal result of this paper. In common with its parent Lévy distribution, the two parameter distribution [Eq. (9)] has divergent integer moments. Although not of the stable class, this distribution is infinitely divisible, and this property has implications for explaining some features in data that follows.

The asymptotic behavior of the distribution [Eq. (9)] can be deduced for different values of α and γ. When $t\gg 1$ the form adopted by Eq. (9) is similar to that of the Lévy distribution with the same index γ, i.e., $p_{\alpha,\gamma}(t)\sim t^{-\gamma-1}$, giving a scale invariant behavior in this regime. Specifically,

$$p_{\alpha,\gamma}(t)\sim\frac{2\Gamma(1+\gamma)}{\pi}\sin\left(\frac{\pi\gamma}{2}\right)t^{-1-\gamma},\quad 0<\gamma<2,\quad x\gg 1. \tag{10}$$

When $t\ll 1$, the form of the distribution depends upon the size of both γ and the product $\alpha\gamma$ when compared with unity. The important property to note is that the distribution can have either an increasing or decreasing power law at small values of t for particular values of the parameters α and γ. Specifically,

$$p_{\alpha,\gamma}(t)\sim\begin{cases}\dfrac{[\alpha|\cos(\gamma\pi/2)|]^\alpha}{\gamma\Gamma(\alpha,\gamma)}\dfrac{\sin[\alpha\pi(\gamma-1)]}{\sin(\alpha\pi\gamma)}t^{\alpha\gamma-1}, & \alpha\gamma<1,\quad \gamma>1 \quad (11a)\\ \dfrac{[\alpha|\cos(\gamma\pi/2)|]^{1/\gamma}\Gamma(1+1/\gamma)\Gamma[(\alpha\gamma-1)/\gamma]\sin(\pi/\gamma)}{\pi\Gamma(\alpha)}, & \alpha\gamma>1,\quad \gamma>1 \quad (11b)\\ \dfrac{[\alpha|\cos(\gamma\pi/2)|]^\alpha}{\Gamma(\alpha,\gamma)}t^{\alpha\gamma-1}, & \text{all } \alpha\gamma,\quad \gamma<1 \quad (11c)\\ \dfrac{1}{2}\left(\dfrac{\cos(\gamma\pi/2)}{\gamma}\right)^{1/\gamma}, & \alpha\gamma=1,\quad \gamma<1 \quad (11d)\\ -\dfrac{\sin(\pi/\gamma)}{\pi}\left(\dfrac{|\cos(\gamma\pi/2)|}{\gamma}\right)^{1/\gamma}\ln(t), & \alpha\gamma=1,\quad \gamma>1 \quad (11e)\end{cases}$$

Attention is drawn to the behavior of this distribution in those instances when $\gamma>1$. If $\gamma>1$ and $\alpha\gamma<1$, the distribution possesses two separate power-law behaviors, in the tail with $p_{\alpha,\gamma}(t)\sim t^{-\gamma-1}$ and at small values of t where $p(t)\sim t^{\alpha\gamma-1}$, [Eq. (11a)]. If $\alpha\gamma>1$ the distribution retains its power-law tail but has an inner scale [Eq. (11b)].

The effect of finite $\overline{N}$ is to modify the distribution, so that the PDF is now.

$$p_{\overline{N}}(t)=\mathrm{Re}\frac{1}{\pi}\int_0^\infty\left[1+\frac{\overline{N}}{\alpha}[1-\exp(-u^\gamma(1+i\Lambda)/\overline{N})]\right]^{-\alpha}\times\exp(iut)du, \tag{12}$$

which has three parameters: $\overline{N},\gamma$, and α. An analysis identical to that shown in Ref. [5] reveals that $\overline{N}$ introduces an inner scale which resolves the inner power law that occurs when $\alpha\gamma<1$. This inner scale extends out to $t\sim\gamma(\overline{N})^{-1/\gamma}$. Beyond this region, the PDF matches the inner power-law of the limit distribution, whereupon the two distributions become indistinguishable.

Figure 7 shows the trapping-time distribution obtained from the cellular automaton, which has a power-law tail of index $\nu_t=-2.16$, so that $\gamma=-1.16$, indicated by the dashed curve. This, together with the information derived from Fig. 5, $\overline{N}=80$ and $\alpha=0.2$, enables one to obtain all the parameters required to apply distributions (9) and (12). For $\overline{N}\sim 80$, the inner scale occurs at $t\sim 0.027$.

Asymptotes (10) and (11a), that predict the power-law indices ν_t and ν_f, associated with the tail and 'front' of the distribution, respectively, are connected through the cluster parameter by

$$\nu_f+\alpha\nu_t+1+\alpha=0. \tag{13}$$

Relationship (13) allows one to make a comparison between distribution (9) and the temporal behavior observed in the cellular automaton. The dot-dashed curve in Fig. 7 shows the trapping-time distribution derived from the cellular automaton [4] for a sand pile of length $L=400$. Although sand piles with $L>400$ were studied in Ref. [4], these revealed no new features. From Fig. 7 the indices of the tail and front power laws are $\nu_t=-2.16$ and $\nu_f=-0.78$, which, on using Eq. (13), give $\gamma=1.16$ and $\alpha=0.2$ as parameters for distribution (9). The value for α is in accord with the value of the cluster parameter obtained for the number fluctuations. The limit distribution [Eq. (9)] is also shown in Fig. 7 by a full line. The chain line is data obtained from the cellular automaton, which is scaled linearly according to $p(t)\rightarrow 50p(t/80)$. The limit distribution [Eq. (9)] overestimates the number of very short trapping times, since it assumes the existence of an infinite number of arbitrarily small step lengths. Figure 6 indicates that $\overline{N}\sim 80$, which, although large, is finite. The dotted line in Fig. 7 shows the distribution [Eq. (12)] with $\overline{N}\sim 80$. This has the same asymptotic behavior, but an inner scale resolves the small-scale power law.

Figure 3 of Ref. [4] showed the transit-time distribution for grains passing through the entire pile. This has the same tail as the distribution for trapping times, but is constant for small transit times, i.e., it exhibits an inner scale for short transit times. This behavior is readily understood in terms of the model presented here, since the transit time is the independent sum of individual trapping times. The characteristic function of the distribution of the transit times is of the same form as that in Eq. (9) by virtue of infinite divisibility, but with different parameter, viz.

$$[1+u^{\gamma}(1+i\Lambda)/\alpha]^{-\overline{M}\alpha},$$

with $\overline{M}$ the average number of trappings on the long time scale that a grain experiences before being expelled from the pile. This distribution has the same power-law asymptotic form for large values of t as in Eq. (10). The behavior for small values of t depends on the value of $\overline{M}$ which can be estimated from Eq. (6). $\overline{M}$ is greater than unity for systems of size $L>40$, but $\overline{M}\alpha\gamma>1$ for system sizes $L>175$. Thus for system sizes greater than ~ 175, the transit-time distribution will exhibit an inner scale, and this is verified by the automaton simulations.

V. SUMMARY AND CONCLUSIONS

This paper has applied diagnostics to a rice-pile simulation. These diagnostics have indicated that the spatial and temporal behaviors of tracer grains can be described in terms of random walk models. Crucially these random walks require the incorporation of step number fluctuations into their formulation. The first model describes the distribution for the resultant flight lengths of grains. This is shown to comprise a sum of relatively short subflights whose number fluctuates according to a discrete power law. The index of the power law describing the resultant flight lengths is inherited from the number fluctuation distribution. The second model describes a temporal quantity, the distribution of times that a grain remains at rest before being transported to another site by an avalanche. The mechanism at work here is more subtle, and relies on the height of the pile fluctuating at a particular site, and thereby bringing a tracer grain to the surface at particular times. The distribution of times between such returns to the surface can be modeled with a one-sided Lévy distribution. The number of times a grain returns to the surface before being transported to another site is described accurately by a negative binomial distribution, and so a trapping time comprises a sum of Lévy distributed step lengths which fluctuate in number. The power-law tail of the trapping time distribution is inherited from the individual Lévy steps which correspond to the distribution of those times when a grain is buried and so cannot move. The index for the tail of the distribution is intimately related to the form of the height fluctuations, and can be quantitatively determined; however, this calculation itself requires distinct innovations, and so the details are presented elsewhere [12]. Features of the distribution occurring at small times are governed by the clustering introduced by the number fluctuations.

There are several routes via which this work can be extended and exploited. A technical study of the properties of clustered Lévy random walks formed in higher dimensions and from a finite number of steps was presented elsewhere [5]. A random walk with a power-law distributed number of steps is novel and warrants further investigation. For example, the value of the index β will affect the rate of convergence to either a Gaussian distribution or other stable distributions. The properties of such random walks either on the line or in higher dimensions is of relevance to the study of macroscopic transport phenomena. Analyzing the flights made by tracer particles down SOC profiles can provide a paradigm for motion through unstable or turbulent media, and thereby elucidate aspects of anomalous transport in complex systems. At a deeper level, the stochastic processes which create *discrete* power distributions are of intrinsic and fundamental interest. The mechanism by which power-law behavior is manifested in temporal properties of the pile has been linked to the classical problem of ''first return'' of a stochastic process.

Earlier work produced by a large collective of authors showed how simple cellular automata can reproduce some of the effects observed in the evolution of sand piles. Such work has helped to identify the microscopic mechanisms that may play an important but hidden role in determining the cooperative behavior of complex systems. Adopting a principally computational approach has not, however, provided much physical insight into the processes taking place. This paper has performed a detailed analysis of the statistics of both microscopic transitions and macroscopic changes in a sand pile. In so doing it has revealed patterns of behavior which are amenable to physical interpretation and for which stochastic models either exist or can be developed. With regard to these developments, the discrete power-law distribution provides a potentially fruitful vein for further investigation. The construction of models describing processes whose equilibrium or limiting forms have these unusual statistics

warrants further study, since these processes evidently underpin the dynamics of SOC behavior at the deepest level [13].

ACKNOWLEDGMENTS

It is a pleasure to acknowledge Dr. Á. Corral's clarifications of some details in Ref. [4]. We thank Dr. J. P. Graves, who assisted in the preparation of this paper. This work was supported by the U.K. Engineering and Physical Science Research Council and the Leverhulme Trust.

APPENDIX A

This appendix contains an asymptotic analysis of the spatial random walk for the flight lengths. This requires evaluation of the PDF [Eq. (3)],

$$p(x)=\frac{\exp(-x)}{\zeta(\beta)}\sum_{N_s=0}^{\infty}\frac{x^{N_s}}{N_s!(1+N_s)^{\beta}}$$

which, with the aid of Stirling's formula to represent $N_s!$, can be approximated by the integral

$$p(x)=\frac{1}{\zeta(\beta)(2\pi)^{1/2}}\int_0^{\infty}\frac{\exp[y\ln(x)+y-y\ln(y)-x]dy}{y^{1/2}(1+y)^{\beta}}.$$

The argument of the exponential function has a single turning point at $y=x$, where the numerator of the integrand attains a maximum value of unity. The value of the integral will therefore be dominated by the behavior of the integrand in the vicinity of $y=x$. Expanding the argument of the exponential function to second order about this point leads to the approximation

$$\exp[-(y-x)^2/2y],$$

which possesses the correct behavior near $y=x$ when x is large. Setting $y=(1+u)x$ and considering $x\gg 1$ obtains

$$p(x)=\frac{x^{1/2-\beta}}{\zeta(\beta)(2\pi)^{1/2}}\int_{-1}^{\infty}\frac{\exp\{-xu^2/[2(1+u)]\}du}{(1+u)^{\beta+1/2}}.$$

This integral is in a form that is amenable to the analysis given in Ref. [11], whereupon the first two terms in the expansion are readily found to be those given by Eq. (5) in the text. It is simple to show that, for small values of x,

$$p(x)\sim\frac{1}{\zeta(\beta)}\left[1-x\left(1-\frac{1}{2^{\beta}}\right)+\frac{x^2}{2}\left(1+\frac{1}{3^{\beta}}-\frac{1}{2^{\beta-1}}\right)+\cdots\right].$$

APPENDIX B

This appendix derives the distribution [Eq. (9)] which describes fluctuations in the random variable

$$t=\sum_{m=1}^{N}t_m,$$

where the t_m are independent but statistically identical one-sided Lévy distributed random variables with the characteristic function

$$C_L(u)=\exp\{-|u|^{\gamma}[1+i\,\mathrm{sgn}(u)\Lambda]\},$$

and N fluctuates according to the negative binomial distribution [Eq. (8)]. The average characteristic function that results from considering all realizations of N is

$$C(u)=\sum_{N=0}^{\infty}P(N)C_L(u)^N=\left(1+\frac{\overline{N}}{\alpha}[1-C_L(u)]\right)^{-\alpha}$$

and the distribution for $p(t)$ follows on Fourier transforming this. Noting that $C_L(-u)=C_L(u)^*$ obtains

$$p(t)=\mathrm{Re}\frac{1}{\pi}\int_0^{\infty}du\,\exp(iut)C(u),$$

which is the distribution [Eq. (12)]. On rescaling u through $u\to u/\overline{N}^{1/\gamma}$, followed by a scaling in $t\to t\overline{N}^{1/\gamma}$ obtains the distribution [Eq. (12)]; then letting $\overline{N}\to\infty$ obtains the limit distribution [Eq. (9)].

[1] P. Bak, C. Tang, and K. Wiesenfeld, Phys. Rev. Lett. **59**, 381 (1987); Phys. Rev. A **38**, 364 (1988); E.T. Lu and R.J. Hamilton, Astrophys. J. **380**, L89 (1991); K. Christensen and S.R. Nagel, Rev. Mod. Phys. **64**, 321 (1992); S. Mineshige, M. Takeuchi, and H. Nishimori, Astrophys. J. **435**, L125 (1994); H.L. Swinney, Physica D **76**, 70 (1994); D.H. Zanette and P.A. Alemany, Phys. Rev. Lett. **75**, 366 (1995); R.D. Pinto, W.M. Gonąlves, J.C. Sartorelli, and M.J. de Oliveira, Phys. Rev. E **52**, 6896 (1995); B.M. Boghosian, *ibid.* **53**, 4754 (1996); R.O. Dendy and P. Helander, Plasma Phys. Controlled Fusion **39**, 1947 (1997); A. Chessa, H.E. Stanley, A. Vespignani, and S. Zaperi, Phys. Rev. E **59**, R12 (1999); P. Bak, *How Nature Works* (Oxford University Press, Oxford, 1997).

[2] P. Lévy, *Théorie de l'Addition des Variables Aléatories* (Gauthier-Villars, Paris, 1937).

[3] K. Christensen, Á. Corral, V. Frette, J. Feder, and T. Jøssang, Phys. Rev. Lett. **77**, 107 (1996); V. Frette, K. Christensen, A. Mathe-Sørenssen, J. Feder, T. Jøssang, P. Meakin, Nature (London) **379**, 49 (1996).

[4] M. Boguñá and Á. Corral, Phys. Rev. Lett. **78**, 4950 (1997).

[5] K.I. Hopcraft, E. Jakeman, and R.M.J. Tanner, Phys. Rev. E **60**, 5327 (1999).

[6] E. Jakeman and P.N. Pusey, IEEE Trans. Antennas Propag. **AP24**, 806 (1977); *Radar 77* (IEE, London, 1977), p 105; Phys. Rev. Lett. **40**, 546 (1978); E. Jakeman, J. Phys. A **13**, 31 (1980); E. Jakeman and R.J.A. Tough, Adv. Phys. **37**, 471

(1988); E. Jakeman, Pure Appl. Opt. **1**, 784 (1999).
[7] M. Abramowitz and I.A. Stegun, *Handbook of Mathematical Functions*, 9th ed. (Dover, New York, 1970).
[8] M.V. Berry, Philos. Trans. R. Soc. London, Ser. A **273**, 611 (1973).
[9] W. Feller, *An Introduction to Probability and Its Applications*, 2nd ed. (J Wiley, London, 1971), Vols. I and II; M. Ding and W. Yang, Phys. Rev. E **52**, 207 (1995).
[10] M. Evans, N. Hastings, and B. Peacock, *Statistical Distributions*, 2nd ed. (Wiley, New York, 1993).
[11] R.B. Dingle, *Asymptotic Expansions: Their Derivation and Interpretation*. (Academic, London, 1973).
[12] K.I. Hopcraft, R.M.J. Tanner, E. Jakeman, and J.P. Graves, Phys. Rev. E (to be published).
[13] Additional materials including animations of the cellular automaton can be viewed at http://spencer.nott.ac.uk/~etzrt/index.html.